Table B.5.3(a) Maximum Heat Release Rates from Fire Detection Institute Analysis

Commodity	Approximate Values (Btu/sec)
Medium wastebasket with milk cartons	100
Large barrel with milk cartons	140
Upholstered chair with polyurethane foam	350
Latex foam mattress (heat at room door)	1200
Furnished living room (heat at open door)	4000–8000

For SI units, 1 Btu/sec = 1.055 W.

Table B.5.3(b) Characteristics of Ignition Sources (Babrauskas and Krasny [56])

Ignition Source	Typical Heat Output (W)	Burn Time[a] (sec)	Maximum Flame Height (mm)	Flame Width (mm)	Maximum Heat Flux (kW/m^2)
Cigarette 1.1 g (not puffed, laid on solid surface), bone dry					
Conditioned to 50%	5	1,200	—	—	42
Relative humidity	5	1,200	—	—	35
Methenamine pill, 0.15 g	45	90	—	—	4
Match, wooden (laid on solid surface)	80	20–30	30	14	18–20
Wood cribs, BS 5852 Part 2					
No. 4 crib, 8.5 g	1,000	190	—	—	15[d]
No. 5 crib, 17 g	1,900	200	—	—	17[d]
No. 6 crib, 60 g	2,600	190	—	—	20[d]
No. 7 crib, 126 g	6,400	350	—	—	25[d]
Crumpled brown lunch bag, 6 g	1,200	80	—	—	—
Crumpled wax paper, 4.5 g (tight)	1,800	25	—	—	—
Crumpled wax paper, 4.5 g (loose)	5,300	20	—	—	—
Folded double-sheet newspaper, 22 g (bottom ignition)	4,000	100	—	—	—
Crumpled double-sheet newspaper, 22 g (top ignition)	7,400	40	—	—	—
Crumpled double-sheet newspaper, 22 g (bottom ignition)	17,000	20	—	—	—
Polyethylene wastebasket, 285 g, filled with 12 milk cartons (390 g)	50,000	200[b]	550	200	35[c]
Plastic trash bags, filled with cellulosic trash (1.2–14 kg)[e]	120,000–350,000	200[b]	—	—	—

For U.S. units, 1 in. = 25.4 mm; 1 Btu/sec = 1.055 W; 1 oz = 0.02835 kg = 28.35 g; 1 Btu/ft^2-sec = 11.35 kW/m^2.
[a]Time duration of significant flaming.
[b]Total burn time in excess of 1800 seconds.
[c]As measured on simulation burner.
[d]Measured from 25 mm away.
[e]Results vary greatly with packing density.

Table B.5.3(c) Characteristics of Typical Furnishings as Ignition Sources (Babrauskas and Krasny [56])

Furnishings	Total Mass (kg)	Total Heat Content (mJ)	Maximum Rate of Heat Release (kW)	Maximum Thermal Radiation to Center of Floor* (kW/m^2)
Wastepaper baskets	0.73–1.04	0.7–7.3	4–18	0.1
Curtains, velvet, cotton	1.9	24	160–240	1.3–3.4
Curtains, acrylic/cotton	1.4	15–16	130–150	0.9–1.2
TV sets	27–33	145–150	120–290	0.3–2.6
Chair mockup	1.36	21–22	63–66	0.4–0.5
Sofa mockup	2.8	42	130	0.9
Arm chair	26	18	160	1.2
Christmas trees, dry	6.5–7.4	11–41	500–650	3.4–14

For U.S. units, 1 lb = 0.4536 kg = 453.6 g; 1 Btu = 1.055×10^{-3} mJ; 1 Btu/sec = 1.055 kW; 1 $Btu/ft^2 \cdot sec$ = 11.35 kW/m^2.
*Measured at approximately 2 m away from the burning object.

Table B.5.3(d) Heat Release Rates of Chairs (Babrauskas and Krasny [56])

Specimen	kg	Mass Combustible (kg)	Style	Frame	Padding	Fabric	Interliner	Peak *m* (g/sec)	Peak *q* (kW)
C12	17.9	17.0	Traditional easy chair	Wood	Cotton	Nylon	—	19.0	290[a]
F22	31.9	—	Traditional easy chair	Wood	Cotton (FR)	Cotton	—	25.0	370
F23	31.2	—	Traditional easy chair	Wood	Cotton (FR)	Olefin	—	42.0	700
F27	29.0	—	Traditional easy chair	Wood	Mixed	Cotton	—	58.0	920
F28	29.2	—	Traditional easy chair	Wood	Mixed	Cotton	—	42.0	730
CO2	13.1	12.2	Traditional easy chair	Wood	Cotton, PU	Olefin	—	13.2	800[b]
CO3	13.6	12.7	Traditional easy chair	Wood	Cotton, PU	Cotton	—	17.5	460[a]
CO1	12.6	11.7	Traditional easy chair	Wood	Cotton, PU	Cotton	—	17.5	260[a]
CO4	12.2	11.3	Traditional easy chair	Wood	PU	Nylon	—	75.7	1350[b]
C16	19.1	18.2	Traditional easy chair	Wood	PU	Nylon	Neoprene	NA	180
F25	27.8	—	Traditional easy chair	Wood	PU	Olefin	—	80.0	1990
T66	23.0	—	Traditional easy chair	Wood	PU, polyester	Cotton	—	27.7	640
F21	28.3	—	Traditional easy chair	Wood	PU (FR)	Olefin	—	83.0	1970
F24	28.3	—	Traditional easy chair	Wood	PU (FR)	Cotton	—	46.0	700
C13	19.1	18.2	Traditional easy chair	Wood	PU	Nylon	Neoprene	15.0	230[a]
C14	21.8	20.9	Traditional easy chair	Wood	PU	Olefin	Neoprene	13.7	220[a]
C15	21.8	20.9	Traditional easy chair	Wood	PU	Olefin	Neoprene	13.1	210[b]
T49	15.7	—	Easy chair	Wood	PU	Cotton	—	14.3	210
F26	19.2	—	Thinner easy chair	Wood	PU (FR)	Olefin	—	61.0	810
F33	39.2	—	Traditional loveseat	Wood	Mixed	Cotton	—	75.0	940

(continues)

Table B.5.3(d) *(Continued)*

Specimen	kg	Mass Combustible (kg)	Style	Frame	Padding	Fabric	Interliner	Peak *m* (g/sec)	Peak *q* (kW)
F31	40.0	—	Traditional loveseat	Wood	PU (FR)	Olefin	—	130.0	2890
F32	51.5	—	Traditional sofa	Wood	PU (FR)	Olefin	—	145.0	3120
T57	54.6	—	Loveseat	Wood	PU, cotton	PVC	—	61.9	1100
T56	11.2	—	Office chair	Wood	Latex	PVC	—	3.1	80
CO9/T64	16.6	16.2	Foam block chair	Wood (part)	PU, polyester	PU	—	19.9	460
CO7/T48	11.4	11.2	Modern easy chair	PS foam	PU	PU	—	38.0	960
C10	12.1	8.6	Pedestal chair	Rigid PU foam	PU	PU	—	15.2	240[a]
C11	14.3	14.3	Foam block chair	—	PU	Nylon	—	NA	810[b]
F29	14.0	—	Traditional easy chair	PP foam	PU	Olefin	—	72.0	1950
F30	25.2	—	Traditional easy chair	Rigid PU foam	PU	Olefin	—	41.0	1060
CO8	16.3	15.4	Pedestal swivel chair	Molded PE	PU	PVC	—	112.0	830[b]
CO5	7.3	7.3	Bean bag chair	—	Polystyrene	PVC	—	22.2	370[a]
CO6	20.4	20.4	Frameless foam back chair	—	PU	Acrylic	—	151.0	2480[b]
T50	16.5	—	Waiting room chair	Metal	Cotton	PVC	—	NA	<10
T53	15.5	1.9	Waiting room chair	Metal	PU	PVC	—	13.1	270
T54	27.3	5.8	Metal frame loveseat	Metal	PU	PVC	—	19.9	370
T75/F20	7.5(×4)	2.6	Stacking chairs (4)	Metal	PU	PVC	—	7.2	160

For U.S. units, 1 lb/sec = 0.4536 kg/sec = 453.6 g/sec; 1 lb = 0.4536 kg; 1 Btu/sec = 1.055 kW.
[a]Estimated from mass loss records and assumed Wh_c.
[b]Estimated from doorway gas concentrations.

Table B.5.3(e) Effect of Fabric Type on Heat Release Rate in Table B.5.3(a) (Within Each Group All Other Construction Features Kept Constant) (Babrauskas and Krasny [56])

Specimen	Full-Scale Peak *q* (kW)	Padding	Fabric
	Group 1		
F24	700	Cotton (750 g/m^2)	FR PU foam
F21	1970	Polyolefin (560 g/m^2)	FR PU foam
	Group 2		
F22	370	Cotton (750 g/m^2)	Cotton batting
F23	700	Polyolefin (560 g/m^2)	Cotton batting
	Group 3		
28	760	None	FR PU foam
17	530	Cotton (650 g/m^2)	FR PU foam
21	900	Cotton (110 g/m^2)	FR PU foam
14	1020	Polyolefin (650 g/m^2)	FR PU foam
7, 19	1340	Polyolefin (360 g/m^2)	FR PU foam

For U.S. units, 1 lb/ft^2 = 48.83 g/m^2; 1 oz/ft^2 = 305 g/m^2; 1 Btu/sec = 1.055 kW.

Table B.5.3(f) Effect of Padding Type on Maximum Heat Release Rate in Table B.5.3(d) (Within Each Group All Other Construction Features Kept Constant) (Babrauskas and Krasny [56])

Specimen	Full-Scale Peak q (kW)	Padding	Fabric
	Group 1		
F21	1970	FR PU foam	Polyolefin (560 g/m^2)
F23	1990	NFR PU foam	Polyolefin (560 g/m^2)
	Group 2		
F21	1970	FR PU foam	Polyolefin (560 g/m^2)
F23	700	Cotton batting	Polyolefin (560 g/m^2)
	Group 3		
F24	700	FR PU foam	Cotton (750 g/m^2)
F22	370	Cotton batting	Cotton (750 g/m^2)
	Group 4		
12, 27	1460	NFR PU foam	Polyolefin (360 g/m^2)
7, 19	1340	FR PU foam	Polyolefin (360 g/m^2)
15	120	Neoprene foam	Polyolefin (360 g/m^2)
	Group 5		
20	430	NFR PU foam	Cotton (650 g/m^2)
17	530	FR PU foam	Cotton (650 g/m^2)
22	0	Neoprene foam	Cotton (650 g/m^2)

For U.S. units, 1 lb/ft^2 = 48.83 g/m^2; 1 oz/ft^2 = 305 g/m^2; 1 Btu/sec = 1.055 kW.

Table B.5.3(g) Effect of Frame Material for Specimens with NFR PU Padding and Polyolefin Fabrics (Babrauskas and Krasny [56])

Specimen	Mass (kg)	Peak q (kW)	Frame
F25	27.8	1990	Wood
F30	25.2	1060	Polyurethane
F29	14.0	1950	Polypropylene

For U.S. units, 1 lb = 0.4536 kg; 1 Btu/sec = 1.055 kW.

B.6.3 Ignition. Equations for time to ignition, t_{ig}, are given for both thermally thin and thermally thick materials, as defined in B.6.3.1 and B.6.3.2. For materials of intermediate depth, estimates for t_{ig} necessitate considerations beyond the scope of this presentation (Quintiere [44]; Hirsch [58]).

Table B.5.3(h) Considerations for Selecting Heat Release Rates for Design

Constant Heat Release Rate Fires	Heat Release Rate
Theobald (industrial)	260 kW/m^2 (approx. 26 Btu/sec-ft^2)
Law [22] (offices)	290 kW/m^2 (approx. 29 Btu/sec-ft^2)
Hansell & Morgan [7] (hotel rooms)	249 kW/m^2 (approx. 25 Btu/sec-ft^2)
Variable Heat Release Rate Fires	
NBSIR 88-3695	**Fire Growth Rate**
Fuel Configuration	
Computer workstation	
Free burn	Slow to fast
Compartment	Very slow
Shelf storage	
Free burn	Medium up to 200 sec, fast after 200 sec
Office module	Very slow to medium
NISTIR 483	**Peak Heat**
Fuel commodity:	**Release Rate (kW)**
Computer workstation	1000–1300
NBS Monograph 173	
Fuel commodity:	
Chairs	80–2480 (<10, metal frame)
Loveseats	940–2890 (370, metal frame)
Sofa	3120

For U.S. units, 1 Btu/sec = 1.055 kW.

Table B.6.2(a) Relation of Calorimeter-Measured Properties to Fire Analysis

Property	Ignition	Flame Spread	Fire Size (Energy)
Rate of heat release*		X	X
Mass loss*			X
Time to ignition*	X	X	
Effective thermal properties†	X	X	
Heat of combustion†		X	X
Heat of gasification†			X
Critical ignition flux†	X	X	
Ignition temp.†	X	X	

*Property is a function of the externally applied incident flux.
†Derived properties from calorimeter measurements.

B.6.3.1 Thermally Thin Materials. Relative to ignition from a constant incident heat flux, q_i, at the exposed surface and with relatively small heat transfer losses at the unexposed surface, a thermally thin material is a material whose temperature is relatively uniform throughout its entire thickness, l, at $t = t_{ig}$. For example, at $t = t_{ig\alpha}$:

$$T_{unexposed} BT_o < 0.1\left(T_{exposed} BT_o\right) = 0.1\left(T_{ig} BT_o\right) \quad \textbf{(B.6.3.1a)}$$

Equation B.6.3.1a can be used to show that a material is thermally thin (Hirsch [58]) if:

$$1 < 0.6\left(t''_{ig}\right)^{1/2} \quad \textbf{(B.6.3.1b)}$$

Table B.6.2(b) Average Maximum Heat Release Rates (kW/m²)

Material	Orientation	2.2 Btu/sec/ft² (25 kW/m²) Exposing Flux	4.4 Btu/sec/ft² (50 kW/m²) Exposing Flux	6.6 Btu/sec/ft² (75 kW/m²) Exposing Flux
PMMA	Horizontal	57	79	114
	Vertical	49	63	114
Pine	Horizontal	12	21	23
	Vertical	11	15	56
Sample A	Horizontal	11	18	22
	Vertical	8	11	19
Sample B	Horizontal	12	15	21
	Vertical	5.3	18	29
Sample C	Horizontal	—	19	22
	Vertical	—	15	15
Sample D	Horizontal	6.2	13	13
	Vertical	—	11	11

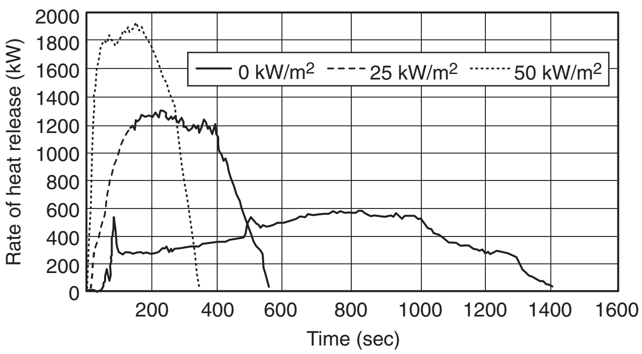

FIGURE B.6.2 Typical Graphic Output of Cone Calorimeter Test.

For example, for sheets of maple or oak wood (where the thermal diffusivity = 1.28 × 10-7 m²/sec; Sako and Hasemi [59]), if t_{ig} = 35 seconds is measured in a piloted ignition test, then, according to Equation B.6.3.1b, if the sample thickness is less than approximately 0.0013 m, the unexposed surface of the sample can be expected to be relatively close to T_{ig} at the time of ignition, and the sample is considered to be thermally thin.

The time to ignition of a thermally thin material subjected to incident flux above a critical incident flux is as follows:

$$t_{ig} = \rho c l \frac{\left(T_{ig} - T_o\right)}{\dot{q}_i''} \qquad \textbf{(B.6.3.1c)}$$

B.6.3.2 Thermally Thick Materials. Relative to the type of ignition test described in B.6.3.1, a sample of a material of a thickness, *l*, is considered to be thermally thick if the increase in temperature of the unexposed surface is relatively small compared to that of the exposed surface at $t = t_{ig}$. For example, at $t = t_{ig}$:

$$t_{ig} = \rho c l \frac{\left(T_{ig} - T_o\right)}{\dot{q}_i''} \qquad \textbf{(B.6.3.2a)}$$

Equation B.6.3.2a can be used to show that a material is thermally thick (Carslaw and Jaeger [60]) if

$$T_{unexposed} B T_o < 0.1\left(T_{exposed} B T_o\right) = 0.1\left(T_{ig} B T_o\right) \qquad \textbf{(B.6.3.2b)}$$

For example, according to Equation B.6.3.2b, in the case of an ignition test on a sheet of maple or oak wood, if t_{ig} = 35 seconds is measured in a piloted ignition test, then, if the sample thickness is greater than approximately 0.0042 m, the unexposed surface of the sample can be expected to be relatively close to T_o at $t = t_{ig}$ and the sample is considered to be thermally thick.

Time to ignition of a thermally thick material subjected to incident flux above a critical incident flux is as follows:

$$l > 2\left(t_{ig} 10\right)^{1/2} \qquad \textbf{(B.6.3.2c)}$$

It should be noted that a particular material is not intrinsically thermally thin or thick (i.e., the characteristic of being thermally thin or thick is not a material characteristic or property) but also depends on the thickness of the particular sample (i.e., a particular material can be implemented in either a thermally thick or thermally thin configuration).

B.6.3.3 Propagation Between Separate Fuel Packages. Where the concern is for propagation between individual separated fuel packages, incident flux can be calculated using traditional radiation heat transfer procedures (Tien, Lee, and Stretton [61]).

The rate of radiation heat transfer from a flaming fuel package of total energy release rate, *Q*, to a facing surface element of an exposed fuel package can be estimated from the following:

$$q''_{inc} = \frac{X_r Q}{4\pi r^2} \qquad \textbf{(B.6.3.3)}$$

where:
q''_{inc} = incident flux on exposed fuel
X_r = radiant fraction of exposing fire
Q = rate of heat release of exposing fire
r = radial distance from center of exposing fire to exposed fuel

B.6.4 Estimating Rate of Heat Release. As discussed in B.6.2, tests have demonstrated that the energy feedback from a burning fuel package ranges from approximately 25 kW/m² to 50 kW/m². For a reasonable conservative analysis, it is recommended that test data developed with an incident flux of 50 kW/m² be used. For a first-order approximation, it should be assumed that all the surfaces that can be simultaneously involved in burning are releasing energy at a rate equal to that determined by testing the material in a fire properties calorimeter with an incident flux of 50 kW/m² for a free-burning material and 75 kW/m² to 100 kW/m² for post-flashover conditions.

In making this estimate, it is necessary to assume that all surfaces that can "see" an exposing flame (or superheated gas, in the post-flashover condition) are burning and releasing energy and mass at the tested rate. If sufficient air is present, the rate of heat release estimate is then calculated as the product of the exposed area and the rate of heat release per unit area as determined in the test calorimeter. Where there are test data taken at the incident flux of the exposing flame, the tested rate of heat release should be used. Where the test data are for a different incident flux, the burning rate should be estimated using the heat of gasification as expressed in Equation B.6.4a to calculate the mass burning rate per unit area:

$$\dot{m}'' = \frac{\dot{q}_i''}{h_c} \tag{B.6.4a}$$

The resulting mass loss rate is then multiplied by the derived effective heat of combustion and the burning area exposed to the incident flux to produce the estimated rate of heat release as follows:

$$\dot{Q}_i'' = \dot{m}'' h_c A \tag{B.6.4b}$$

B.6.5 Flame Spread. If it is desired to predict the growth of fire as it propagates over combustible surfaces, it is necessary to estimate flame spread. The computation of flame spread rates is an emerging technology still in an embryonic stage. Predictions should be considered as order-of-magnitude estimates.

Flame spread is the movement of the flame front across the surface of a material that is burning (or exposed to an ignition flame) where the exposed surface is not yet fully involved.

Physically, flame spread can be treated as a succession of ignitions resulting from the heat energy produced by the burning portion of a material, its flame, and any other incident heat energy imposed upon the unburned surface. Other sources of incident energy include another burning object, high temperature gases that can accumulate in the upper portion of an enclosed space, and the radiant heat sources used in a test apparatus such as the cone calorimeter or the LIFT mechanism. For analysis purposes, flame spread can be divided into two categories: that which moves in the same direction as the flame (concurrent or wind-aided flame spread) and that which moves in any other direction (lateral or opposed flame spread). Concurrent flame spread is assisted by the incident heat flux from the flame to unignited portions of the burning material. Lateral flame spread is not so assisted and tends to be much slower in progression unless an external source of heat flux is present. Concurrent flame spread can be expressed as follows:

$$V = \frac{\dot{q}_i'' L}{k\rho c\left(T_{ig} - T_s\right)^2} \tag{B.6.5}$$

The values for $k\rho c$ and ignition temperature are calculated from the cone calorimeter as previously discussed. For this equation, the flame length (L) is measured from the leading edge of the burning region.

B.7 *t*-Squared Fires.

B.7.1 Over the past decade, persons interested in developing generic descriptions of the rate of heat release of accidental open flaming fires have used a "*t*-squared" approximation for this purpose. A *t*-squared fire is one in which the burning rate varies proportionally to the square of time. Frequently, *t*-squared fires are classed by speed of growth, labeled fast, medium, and slow (and occasionally ultra-fast). Where these classes are used, they are defined on the basis of the time required for the fire to grow to a rate of heat release of 1000 Btu/sec. The times related to each of these classes are as shown in Table B.7.1.

Table B.7.1 Time for the Fire Growth Rate to Reach 1000 Btu/sec

Class	Time (sec)
Ultra-fast	75
Fast	150
Medium	300
Slow	600

The general equation is as follows:

$$q = at^2$$

where:
q = rate of heat release (normally in Btu/sec or kW)
a = constant governing the speed of growth
t = time (normally in sec)

B.7.2 Relevance of *t*-Squared Approximation to Real Fires. A *t*-squared fire can be viewed as one in which the rate of heat release per unit area is constant over the entire ignited surface and the fire is spreading as a circle with a steadily increasing radius. In such cases, the burning area increases as the square of the steadily increasing fire radius. Of course, other fires that do not have such a conveniently regular fuel array and consistent burning rate might or might not actually produce a *t*-squared curve. The tacit assumption is that the *t*-squared approximation is close enough for reasonable design decisions.

Figure B.7.2(a) is extracted from NFPA 204, *Standard for Smoke and Heat Venting*. It is presented to demonstrate that most fires have an incubation period in which the fire does not conform to

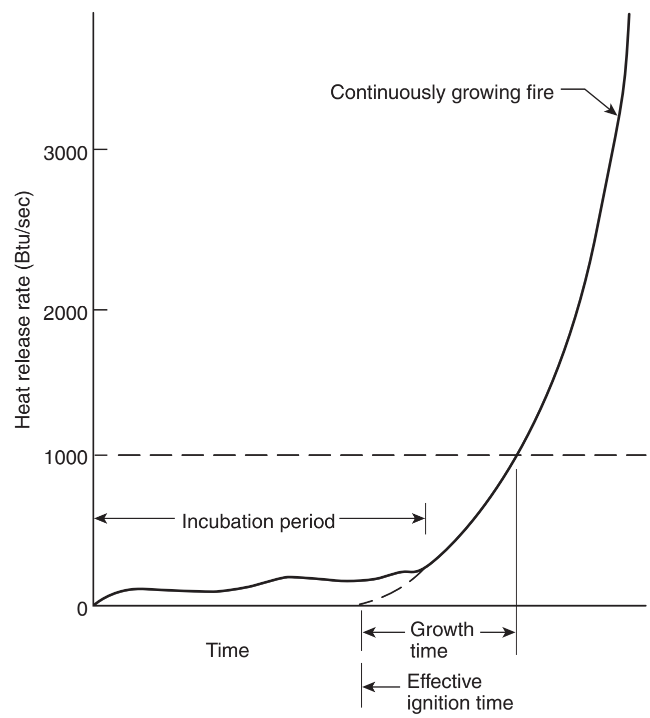

FIGURE B.7.2(a) Conceptual Illustration of Continuous Fire Growth. [204:Figure 8.3.1]

a *t*-squared approximation. In some cases this incubation period can be a serious detriment to the use of the *t*-squared approximation. In most instances, this is not a serious concern in atria and other large spaces covered by this standard. It is expected that the rate of heat release during the incubation period usually would not be sufficient to cause activation of the smoke detection system. In any case, where such activation happens or human observation results in earlier activation of the smoke management system, a fortuitous safeguard would result.

Figure B.7.2(b), extracted from Nelson [62], compares rate of heat release curves developed by the aforementioned classes of *t*-squared fires and two test fires commonly used for test purposes. The test fires are shown as dashed lines labeled "Furniture" and "6 ft storage." The dashed curves farther from the origin show the actual rates of heat release of the test fires used in the development of the residential sprinkler and a standard 6 ft high array of test cartons containing foam plastic pails also frequently used as a standard test fire.

The other set of dashed lines in Figure B.7.2(b) shows these same fire curves relocated to the origin of the graph. This is a more appropriate comparison with the generic curves. As can be seen, the rate of growth in these fires is actually faster than that prescribed for an ultra-fast fire. Such is appropriate for a test fire designed to challenge the fire suppression system being tested.

Figure B.7.2(c) relates the classes of *t*-squared fire growth curves to a selection of actual fuel arrays from NFPA 204. The individual arrays are also described in Annex B.

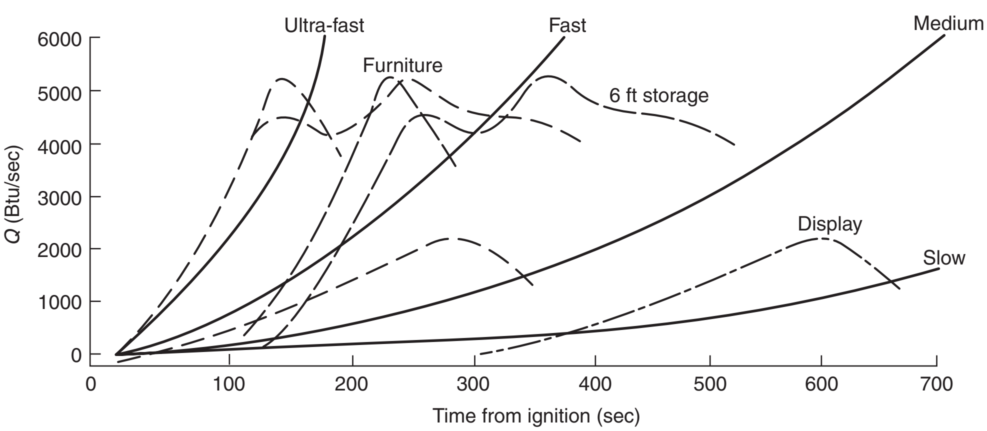

FIGURE B.7.2(b) Rates of Energy Release in a *t*-Squared Fire. (Source: Nelson [62])

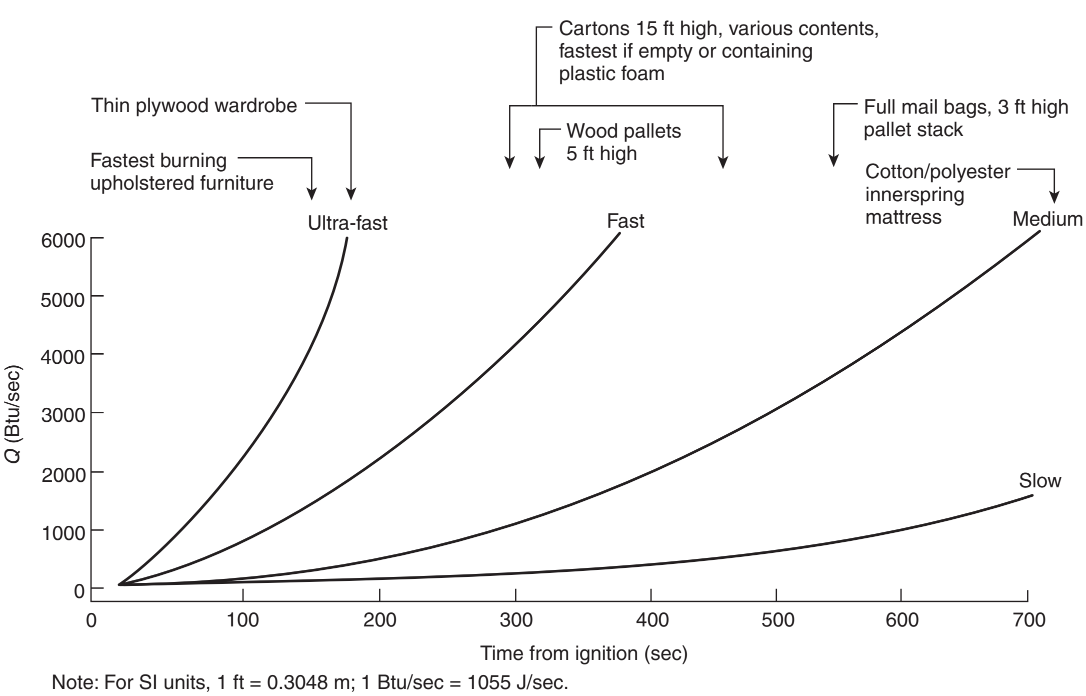

FIGURE B.7.2(c) Relation of *t*-Squared Fire to Some Fire Tests.

Annex C Computer-Based Models for Atria and Malls

This annex is not a part of the requirements of this NFPA document but is included for informational purposes only.

C.1 Zone Fire Models

C.1.1 Overview. Smoke produced from a fire in a large, open space is assumed to be buoyant, rising in a plume above the fire and striking the ceiling or stratifying due to temperature inversion. After the smoke either strikes the ceiling or stratifies, the space can be expected to begin to fill with smoke, with the smoke layer interface descending. The descent rate of the smoke layer interface depends on the rate at which smoke is supplied to the smoke layer from the plume. Such smoke filling is represented by a two-zone model in which there is a the ambient air. For engineering purposes, the smoke supply rate from the plume can be estimated to be the air entrainment rate into the plume below the smoke layer interface.

Sprinklers can reduce the heat release rate and the air entrainment rate into the plume.

As a result of the zone model approach, the model assumes uniform properties (smoke concentration and temperature) from the point of interface through the ceiling and horizontally throughout the entire smoke layer.

For general information about fire plumes and ceiling jets, see Beyler [2].

C.1.2 Simplifications of Zone Fire Models. Zone models are simple models and can usually be run on personal computers. Zone models divide the space into two zones, an upper zone, which contains the smoke and hot gases produced by the fire, and a lower zone, which is the source of entrainment air. The sizes of the two zones vary during the course of a fire, depending on the rate of flow from the lower to the upper zone, the rate of exhaust of the upper zone, and the temperature of the smoke and gases in the upper zone. Because of the small number of zones, zone models use engineering equations for heat and mass transfer to evaluate the transfer of mass and energy from the lower zone to the upper zone, the heat and mass losses from the upper zone, and other features. Generally, the equations assume that conditions are uniform in each zone.

In zone models, the source of the flow into the upper zone is the fire plume. All zone models have a plume equation. A few models allow the user to select among several plume equations.

Most current zone models are based on an axisymmetric plume.

Because zone models assume that there is no pre-existing temperature variation in the space, they cannot directly handle stratification. Zone models also assume that the ceiling smoke layer forms instantly and evenly from wall to wall, which fails to account for the initial lateral flow of smoke across the ceiling. The resulting error can be significant in spaces having large ceiling areas. Zone models can, however, calculate many important factors in the course of events (e.g., smoke level, temperature, composition, and rate of descent) from any fire that the user can describe. Most zone models will calculate the extent of heat loss to the space boundaries. Several models calculate the impact of vents or mechanical exhaust, and some predict the response of heat- or smoke-actuated detection systems.

Common simplifications of zone models are listed as follows:

(1) Fuel
  (a) Heat release rate is not accelerated by heat feedback from smoke layer.
  (b) Post-flashover heat release rate is weakly understood, and its unique simulation is attempted by only a few models.
  (c) CO production is simulated, but its mechanism is not fully understood through the flashover transition.
  (d) Some models do not consider burning of excess pyrolyzate on exit from a vent.
(2) Plumes
  (a) Plume mass entrainment is ±20 percent and not well verified in tall compartments.
  (b) There is no transport time from the fire elevation to the position of interest in the plume and ceiling jet.
  (c) Spill plume models are not well developed.
  (d) Not all plume models consider the fuel area geometry.
  (e) Entrainment along stairwells is not simulated.
  (f) Entrainment from horizontal vents is not simulated by all models.
(3) Layers
  (a) Hot stagnation layers at the ceiling are not simulated.
  (b) There is uniformity in temperature.
(4) Heat transfer
  (a) Some models do not distinguish between thermally thin and thermally thick walls.
  (b) There is no heat transfer via barriers from room to room.
  (c) Momentum effects are neglected.
(5) Ventilation: Mixing at vents is correlationally determined.

C.1.3 Nonuniform Spaces.

C.1.3.1 Sensitivity Analysis. In the absence of an analysis using scale models, field models, or zone model adaptation, a sensitivity analysis should be considered. A sensitivity analysis can provide important information to assist in engineering judgments regarding the use of Equations 5.4.2.1 and 5.4.2.2 for complex and nonuniform geometries. An example of a sensitivity analysis for a large space having a nonflat ceiling geometry follows.

The first step of the analysis would be to convert a nonuniform geometry to a similar or volume-equivalent uniform geometry.

In the case of the geometry shown in Figure C.1.3.1(a), this would be done as follows:

(1) Convert the actual nonrectangular vertical cross-sectional area to a rectangular vertical cross section of equal area.
(2) The height dimension corresponding to the equivalent rectangular cross section would then be used as a substitute height factor H_{sub} in Equation 5.4.2.2.

Results of Equation 5.4.2.2 should be compared with other minimum and maximum conditions as indicated by Figure C.1.3.1(b).

An appropriate method of comparison could be a graph of Equation 5.4.2.2 as shown in Figure C.1.3.1(c). Assume that the building in question can be evacuated in 3 minutes and that the design criteria require the smoke layer to remain available 10 ft above the floor at this time. A review of the curves would indicate that the smoke layer heights as calculated for the substitute case are appropriate. This conclusion can be drawn by noting that neither the extreme minimum height case (H = 30 ft, W = 60 ft) nor the maximum height case (H = 60 ft) offers an expected answer, but the results for two cases (H = 41.6 ft, W = 60 ft; and H = 30 ft, W = 83.3 ft) can be judged to reasonably approximate the behavior of the nonuniform space. It might otherwise be unreasonable to expect the behavior indicated by the maximum or minimum cases.

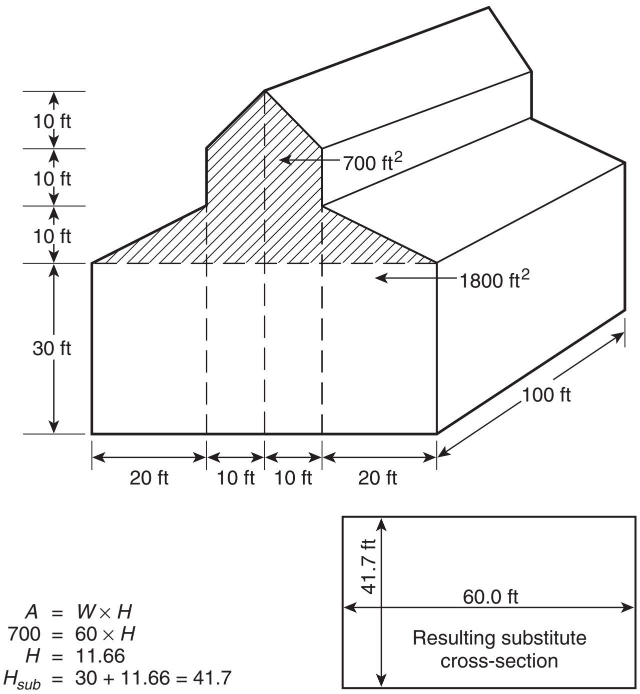

$A = W \times H$
$700 = 60 \times H$
$H = 11.66$
$H_{sub} = 30 + 11.66 = 41.7$

Note: For SI units, 1 ft = 0.3048 m; 1 ft² = 0.0929 m².

FIGURE C.1.3.1(a) Large Space with Nonflat Ceiling.

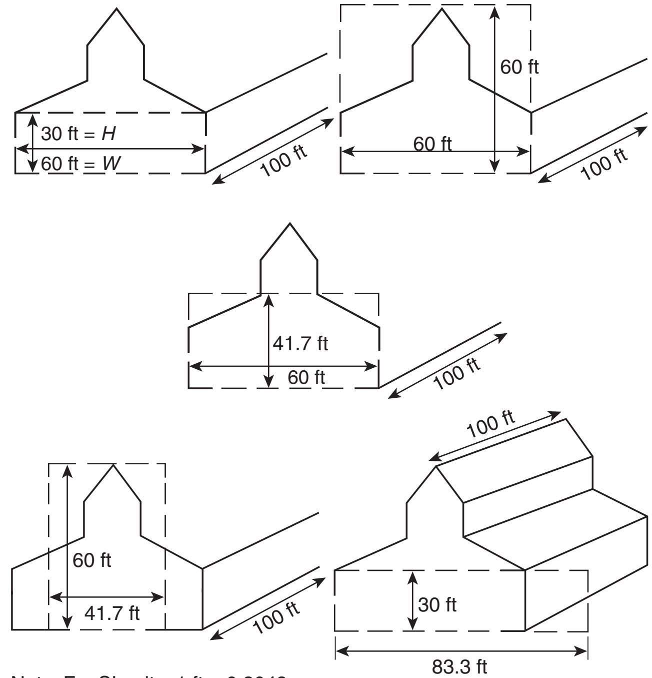

Note: For SI units, 1 ft = 0.3048 m.

FIGURE C.1.3.1(b) Other Nonuniform Geometry Considerations.

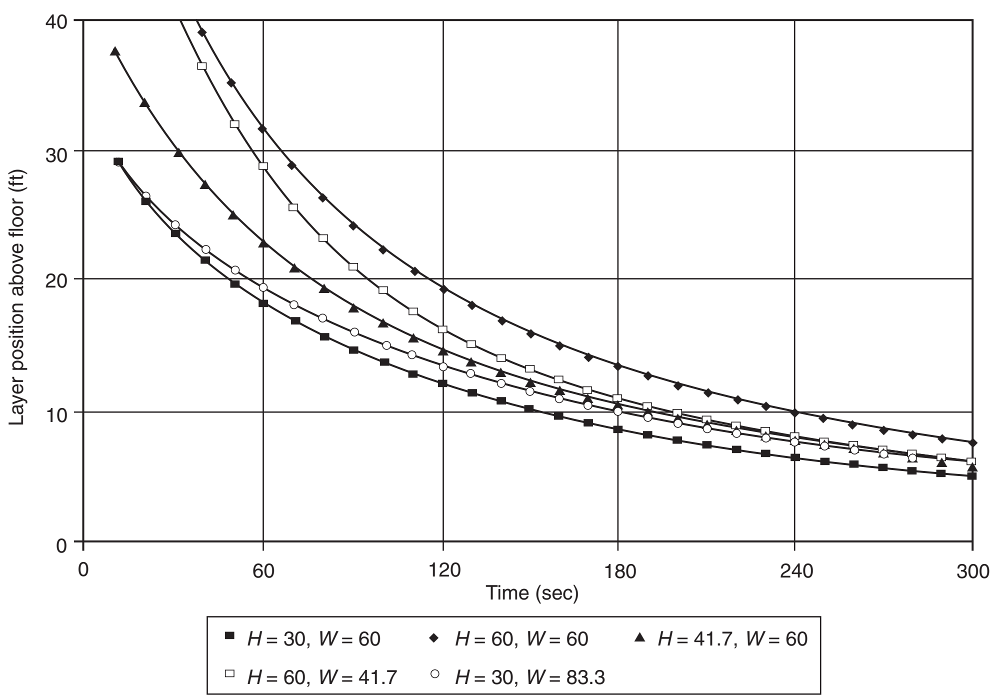

Note: For SI units, 1 ft = 0.3048 m.

FIGURE C.1.3.1(c) Comparison Data for Guidance on Nonrectangular Geometries — Growing Fire.

C.1.3.2 Zone Model Adaptation. A zone model predicated on smoke filling a uniform cross-sectional geometry is modified to recognize the changing cross-sectional areas of a space. The entrainment source can be modified to account for expected increases or decreases in entrainment due to geometric considerations, such as projections.

C.1.3.3 Bounding Analysis. An irregular space is evaluated using maximum height and minimum height identifiable from the geometry of the space using equivalent height or volume considerations.

C.1.4 Zone Fire Model Using Algebraic Equations. A computer model (written in a programming language or using a spreadsheet) can be constructed using the algebraic equations contained in Chapter 5 to calculate the position of a smoke layer interface over time, with and without smoke exhaust. This approach involves the calculation of the mass flow rate of smoke entering the smoke layer, the temperature of the smoke entering the layer, and the mass flow rate of smoke removed from the smoke layer by mechanical or gravity venting. The steps to calculate the position of the smoke layer interface are as follows:

(1) Select the time interval for the calculation, Δt. *(See Table C.1.4.)*
(2) Determine the design fire (e.g., steady fire, growing fire, growing fire with steady maximum, or other description of heat release rate as a function of time). *(See Section 5.2 for a discussion of design fires.)*

Table C.1.4 The Effect of Time Interval on the Accuracy of Smoke Filling Simulations

Atrium Height, *H*		Cross-Sectional Area, *A*			Steady Fire[a]		Fast *t*-Squared Fire[b]	
ft	m	ft²	m²	Time Interval, Δt (s)	Simulation Time (sec)	Error[c] (%)	Simulation Time (sec)	Error[c] (%)
				Small Atrium				
30	9.14	1,000	93	0.005	30	0.0	90	0.0
				0.01	30	0.0	90	0.0
				0.05	30	0.2	90	0.1
				0.20	30	1.2	90	0.2
				0.50	30	3.7	90	0.6
				1.00	30	7.7	90	1.2
				5.00	30	65.0	90	6.1
				Small Spread-Out Atrium				
30	9.14	12,000	1,110	0.01	240	0.0	300	0.0
				0.05	240	0.0	300	0.0
				0.20	240	0.1	300	0.1
				0.50	240	0.1	300	0.1
				1.00	240	0.3	300	0.3
				5.00	240	1.5	300	1.5
				20.00	240	6.3	300	6.4
				Large Atrium				
150	45.7	25,000	2,320	0.01	480	0.0	300	0.0
				0.05	480	0.0	300	0.0
				0.20	480	0.0	300	0.1
				0.50	480	0.1	300	0.1
				1.00	480	0.3	300	0.3
				5.00	480	1.4	300	1.4
				20.00	480	6.0	300	5.8
				Large Spread-Out Atrium				
150	44.7	300,000	27,900	0.01	1200	0.0	600	0.0
				0.05	1200	0.0	600	0.0
				0.20	1200	0.0	600	0.0
				0.50	1200	0.0	600	0.0
				1.00	1200	0.0	600	0.0
				5.00	1200	0.1	600	0.2
				20.00	1200	0.2	600	0.7

Note: Calculations were done with AZONE with the following conditions: (1) ambient temperature of 70°F (21°C); (2) constant cross-sectional area; (3) no smoke exhaust; (4) top of fuel at floor level; (5) wall heat transfer fraction of 0.3.

[a]The steady fire was 5000 Btu/sec (5275 kW).

[b]For the *t*-squared fire, the growth time was 150 sec.

[c]The error, δ, is the error of the smoke layer height, z, using the equation $\delta = 100(z_m - z)/z$, where z_m is the value of z at the smallest time interval listed in the table for that atrium size.